

# The Effect of Toner Rheological Properties on Fusing Performance

Masaki Nakamura

Material Research Laboratory, Fuji Xerox Co. Ltd., Kanagawa, Japan

## Abstract

This paper reports relationship between image gloss and resin rheological properties. Image gloss, which is the surface roughness of toner layer fixed with the electro-photographic heat roll fusing process, has been regarded as one of the most important fusing properties for much better copy image quality. Dynamic viscoelastic properties of resin samples from narrow to very broad molecular weight distribution were measured with a sinusoidally oscillatory shear rheometer. The viscoelastic functions were correlated with image gloss of copy samples prepared by toners made of resin samples. Good correlation was found between a well known viscoelastic parameter " $A_G$ " and image gloss. On the basis of this information, a mechanism of image gloss change can be understood in terms of polymer dynamics, since  $A_G$  can be closely related to the longest relaxation time of polymer chains.

## Introduction

In Heat Roll Fusing Process, there are many performances depending on toner properties, for example, low temperature fusing, high hot offset temperature, releasability from fuser roll surface, image gloss and transparency of color image. In particular, image gloss has been regarded as one of the most important fusing properties for much better image quality of hard copy. Mat-finished toner surface which is called "low image gloss", is preferred for Black & White Copy, and gloss-finished one which is called "high image gloss" is preferred for color copy. To satisfy these performances, a molecular structure of toner binder resin is controlled by molecular weight, molecular weight distribution, polymer configuration and so on.

Through the short time in fusing, there occur several rheological phenomena, i.e. sintering toner particles, adhesion of them onto papers and spreading of toner particle and release of molten toner from fuser roll.

Several studies applying rheology to fusing were reported in past days.<sup>1,2,3</sup> S. K. Bhateja, et al., reported the effect of dispersed magnetite powder in single component toner from stress-strain property and stress relaxation<sup>4</sup>. Satoh, et al., reported relationships between the fusing properties (fixing strength, surface roughness and transparency of color image) and viscoelastic functions at single frequency<sup>5</sup>. Hayakawa, et al., reported empirical equations among fusing properties, molecular structures of binder resin, and rheological functions at single frequency<sup>6</sup>. However, no report has been found on frequency dependence of viscoelastic behavior in molten toner.

In view of molecular design for fusing, it is important to understand time-dependent viscoelastic behavior of toner in terms of molecular dynamics through the time of fusing process.

This study deals with relationship between image gloss and resin rheological properties to clarify the mechanism of image gloss change in heat roll fusing process in terms of polymer dynamics.

## Experiment

**Binder Resin.** Styrene-acrylic uncross-linked copolymers with mono-modal molecular weight distribution (MWD), and with bi-modal MWD were used in this experiment. Table I shows polymer properties of the resin samples.

**Toner.** A mixture of 96wt% resin and 4wt% cyan pigment were melt-mixed by banbury mixer. Toner particles were prepared to evaluate an image gloss by jetting, classification and external additive blending.

**Table 1. Tg, Molecular Weights and Types of Molecular Weight Distribution of Resin Samples**

sample	Tg(°C)	Mw × 10 <sup>-4</sup>	Mn × 10 <sup>-3</sup>	Type
M1	65	1.9	8.9	mono-modal
M22	65	3.4	15.0	mono-modal
B1	62	5.5	3.1	bi-modal
B2	62	8.7	3.0	bi-modal
B3	65	18.0	3.5	bi-modal

\*[M1, M22 - Sekisui Chemical Co. Ltd.]

[B1, B2, B3 - Sanyo Chemical Industries, Ltd.]

**Measurement of Rheological Properties.** Rheological properties were measured by sinusoidally oscillatory shear rheometer with parallel plates, Rheometrics RDA-2. Dynamic storage modulus  $G'(\omega)$ ,  $G''(\omega)$  and absolute complex viscosity  $\eta^*$  were measured in the range of temperature and frequency within from 100 to 220°C and from 0.1 to 400 rad/sec. Data of terminal zone for B1, B2 and B3 samples were obtained by WLF superposition Law.

**Fusing Conditions.** Developed image were fused on Fuji Xerox Color paper by soft roll for Fuji Xerox color copy machine. Nip pressure was 6kgf/cm<sup>2</sup>, and Nip width was 6mm. A developed solid image of 0.9~1mg/cm<sup>2</sup> toner weight was fused at contact time 50, 100, and 200msec in roll nip by changing fuser roll speed. A image gloss of fixed toner was measured by Gloss Meter Model GM-26D for 75° by Murakami Color Research Laboratory.

**Toner Temperature.** A toner temperature at fusing was determined by the interpolation from melting points of waxes and fuser roll temperatures.

## Results

Dynamic viscosity  $\eta'$ , Complex viscosity  $\eta^*$ , zero-shear viscosity  $\eta_0$  are defined as follows:

$$\eta'(\omega) = G''(\omega) / \omega \quad (1)$$

$$\eta^*(\omega) = (G'(\omega)^2 + G''(\omega)^2)^{1/2} \quad (2)$$

$$\eta_0 = \lim_{\omega \rightarrow 0} G''(\omega) / \omega = \lim_{\omega \rightarrow 0} \eta'(\omega) \quad (3)$$

where  $\omega$  is angular frequency. A typical example of  $G'(\omega)$  and  $G''(\omega)$  curves for entangled polymer in melt is drawn in Figure 1. The behavior of  $G'(\omega)$  is expressed by glassy, transition, rubbery plateau, and terminal zone as sketched in Figure 1.<sup>7,8</sup>

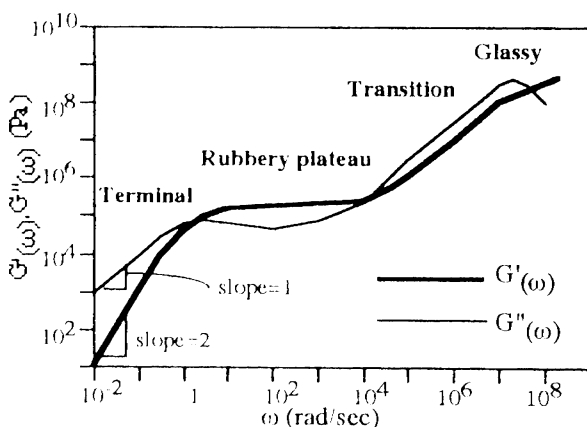


Figure 1. Frequency dependence of  $G'$  and  $G''$  for entangled polymer in melt, illustrating the glassy, transition, rubbery plateau and terminal zone.

Figure 2 shows image gloss plots against toner temperature. In the case of a toner with mono-modal MWD, a image gloss showed a steep increase with toner temperature. On the other hand, in the case of a toner binder with bi-modal MWD, a image gloss showed a gentle slope. Figures 3, 4 and 5 show temperature dependencies of zero-shear viscosity  $\eta_0$ , storage modulus  $G'$  at 10rad/sec, and dynamic viscosity  $\eta'$  at 10 rad/sec, respectively.  $\eta'$  showed similar values in the samples. Temperature dependancies of  $\eta_0$  showed the same slope in the samples, but  $\eta_0$  values were different among the samples. Figures 6 and 7 show frequency dependancies of  $G'$ ,  $G''$  and  $\eta^*$ . It was shown in Figure 6 that M1 resin at 10rad/sec which is nearly the same as the contact time in nip, was in a melt flow state. It was shown in Figure 7 that B3 resin at 10rad/sec was not in the terminal zone.

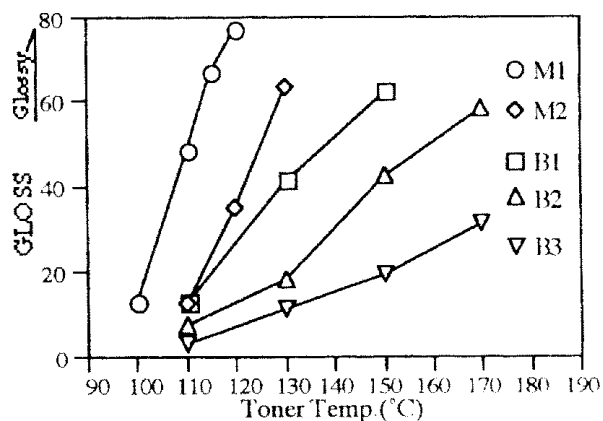


Figure 2. Temperature dependencies of image gloss at contact time 100msec in roll nip for toners of the mono-modal and the bi-modal type resins.

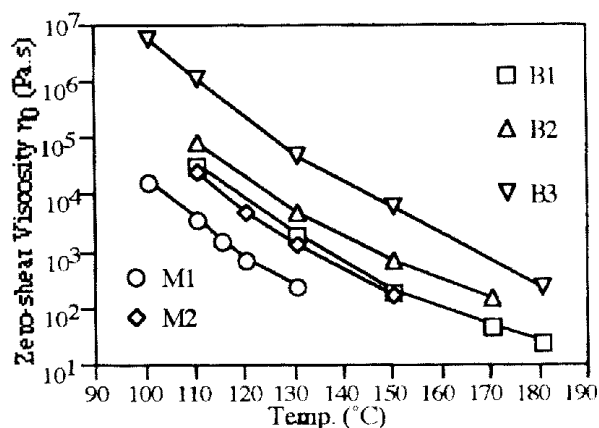


Figure 3. Temperature dependencies of zero-shear viscosity for the mono-modal and the bi-modal type resins.

Steep decrease of  $G'$  on resins M1 and M2 indicate that the resins with mono-modal MWD are in melt flow state in this experiment. Slow decreases of  $G'$  on resins B1, B2 and B3 indicate that the resins with bi-modal MWD are in viscoelastic state.

**Correlation between Image Gloss and Viscoelastic Functions.** Figure 8 shows  $G'$  and  $\eta'$  at 10 rad/sec plots against Image Gloss fused at contact time 100msec in roll nip. Figure 9 shows  $A_G$  and zero-shear viscosity  $\eta_0$  plots against image gloss fused at contact time 100msec in roll nip.  $A_G$  is defined as the infinite frequency limiting value of  $G'$  in terminal zone<sup>7</sup> by equation 4.

$$\lim_{\omega \rightarrow 0} G'(\omega) = A_G \omega^2 \quad (4)$$

$\eta_0$  is defined as a infinite low-frequency limiting value of  $A$  in terminal zone by equation 3. In comparison with Figure 8 and 9,  $A_G$  showed a better fit against Image Gloss. In the same way, good correlations were found between  $A_G$  and image gloss at other contact times 50 and 200msec in roll nip (Figure 10).

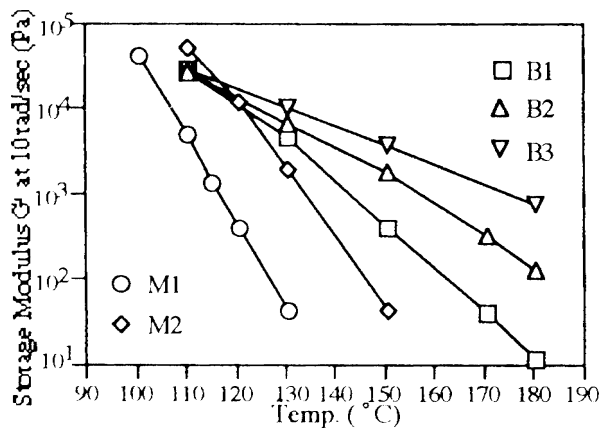


Figure 4. Temperature dependences of  $G'$  at 10 rad/sec for the mono-modal and the bi-modal type resins.

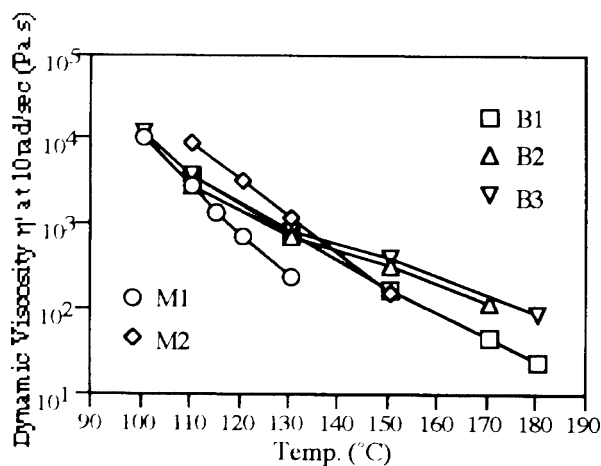


Figure 5. Temperature dependences of  $\eta'$  at 10 rad/sec for the mono-modal and the bi-modal type resins.

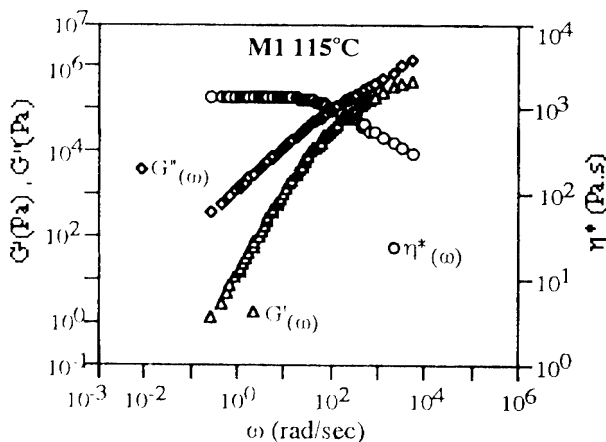


Figure 6. Frequency dependence of  $G'$ ,  $G''$  and complex viscosity for the mono-modal type 1 (M1) at 115°C. Rubbery plateau zone can not be observed.

## Discussion

**Relationships between  $\tau_w$  and Contact Time in Roll NIP.** The weight average relaxation time  $\tau_w$  is defined by Graessley<sup>9</sup>.

$$\tau_w = A_G / \eta_0 \quad (5)$$

$\tau_w$  is regarded as the longest relaxation time of the resin, since  $A_G$  and  $\eta_0$  are determined from terminal zone.

$\tau_w$  of mono-modal resin is regarded as the relaxation time of the longest chain of resin polymer.  $\tau_w$  of bi-modal is regarded as the relaxation time of entanglement of high molecular weight components diluted by low molecular components.  $\eta_0$  may be a friction coefficient of the relaxation.

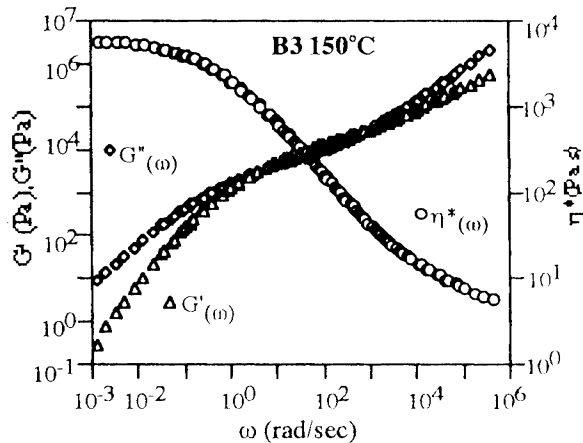


Figure 7. Frequency dependence of  $G'$ ,  $G''$  and complex viscosity for the bi-modal type 3(B3) at 150°C. Rubbery plateau zone can be observed.

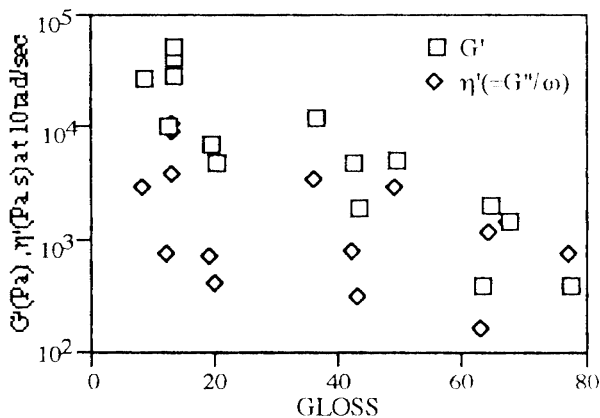


Figure 8.  $G'$  and  $\eta'$  at 10 rad/sec plots against image gloss fixed at contact time 100msec in roll nip.

Contact time in roll nip is considered to be the longest time for relaxation of toner resin in fusing process. Figure 11 shows  $\tau_w$  plots against  $\eta_0$ . In this case, contact time 50msec in roll nip was drawn by the horizontal line in Figure 11.  $A_G$  at image gloss 20, 40 and 60 are obtained from Figure 10, and can be decomposed as functions of  $\tau_w$  and  $\eta_0$ , as shown in Figure 11. In the mono-modal MWD case, image gloss increased to high value because  $\tau_w$  showed less than contact time in roll nip. In the bi-modal MWD case, image gloss becomes low value within the actual fusing temperature because  $\tau_w$  showed much more than the contact time in roll nip.

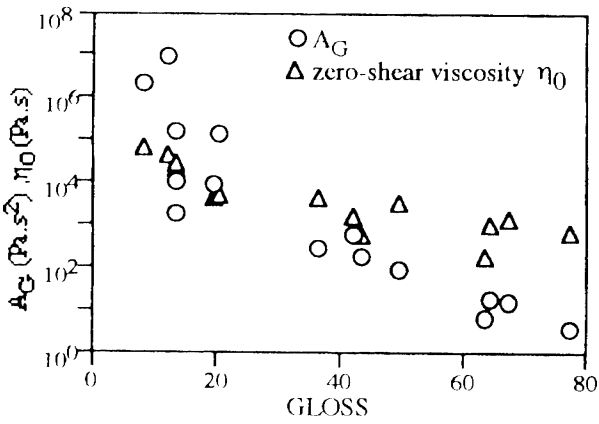


Figure 9.  $A_G$  and  $\eta_0$  plots against image gloss at contact time 10 msec in roll nip.

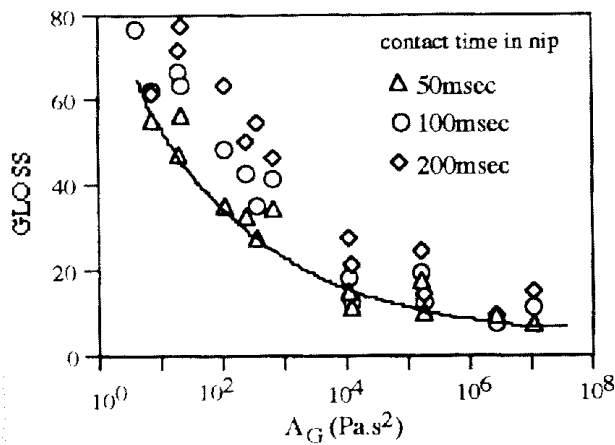


Figure 10. Correlation between  $A_G$  and image gloss at contact times 50, 100 and 200 msec in roll nip.

Therefore, in this experiment, resin rheological behavior in fusing process depend on  $\tau_w$ : when  $\tau_w < \text{contact time}$  in roll nip, the resin rheological behavior is in terminal zone. This means all the entanglements of polymer chains may be undone. When  $\tau_w > \text{contact time}$  in roll nip, the resin rheological behavior is not in terminal zone. This means entanglements may partially remain in polymer chains.

### Conclusion

Image gloss properties in heat roll fusing process can be qualitatively expressed by the time-dependent viscoelastic behavior of binder resin. High image gloss can be gained under the condition that a rheological property of toner resin is in the terminal zone in fusing process.

$A_G (= \tau_w \eta_0)$  shows a good correlation to image gloss. This simple relation will be useful to toner resin design for image gloss control by molecular structure.

The relationship between  $\tau_w$  and image gloss can be explained by the view that contact time in roll nip is equal to the longest time for relaxation of toner resin in fusing process. In consequence, mechanism of image gloss change can be understood in terms of polymer dynamics.

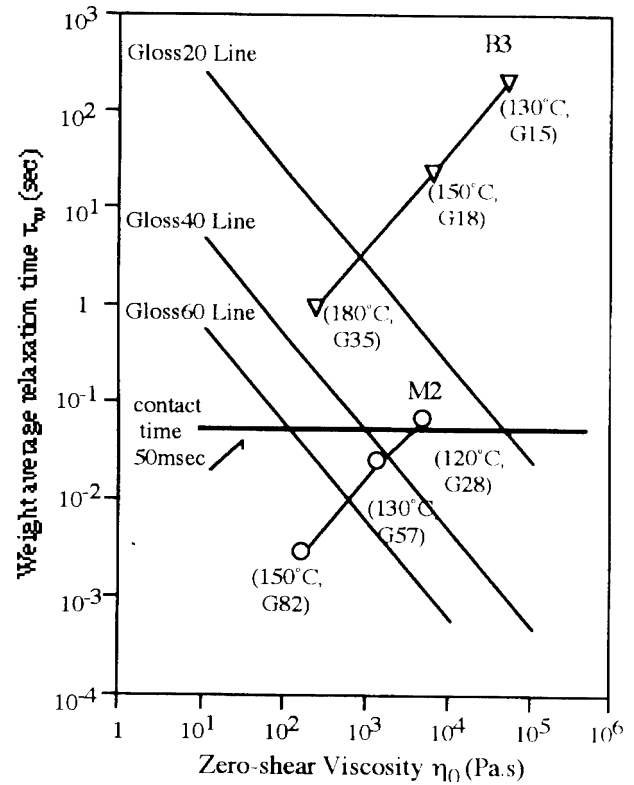


Figure 11. Double-logarithmic plots of  $\tau_w$  and  $\eta_0$  at image gloss 20, 40 and 60.  $A_G$  at these image gloss are obtained from the correlation between  $A_G$  and image gloss at contact time 50 msec in roll nip (Fig. 10).  $\tau_w$  is calculated from equation 5.

### Acknowledgments

I would like to thank to Dr. T. Masuda at Faculty of Engineering Division of Material Chemistry, Kyoto University for his valuable advice. I would like to thank to Sanyo Chemical Industries Ltd., and Sekisui Chemical Co. Ltd. for binder resin samples.

I would like to thank to Mr. K. Tanaka, a manager of Fuji Xerox Co. Ltd., and Mr. K. Takashima, a staff manager of Fuji Xerox Co. Ltd. for their encouragement and discussions to this work.

### References

1. L. H. Lee, "Fixing and Wetting of Xerographic Image on paper-Scanning Electron Microscopy", *Applied Polymer Symposium* No. 23, p. 193.
2. E. M. Williams, "The Physics and Technology of Xerographic Process", John Wiley & Sons, New York.
3. G. Forgo, et al., *J. of Imaging Science and Technology*, vol 37 (1993), No. 2, 176-186.
4. S. K. Bhateja, et al., *J. of Imaging Technology*, Vol. 12, No. 3, June 1986, 156-159.
5. T. Satoh, et al., *J. of Imaging Science*, Vol. 35, No. 6, 1991, 373-376.
6. N. Hayakawa, et al., *IS&T '93 National Congress*, 41-44.
7. J. D. Ferry, "Viscoelastic Properties of Polymers", 3rd Ed., 1980, John Wiley & Sons, New York.
8. T. Masuda, et al., *Macromolecules*, Vol. 14, 354, 1981.
9. W. W. Graessley, "Entanglement Concept in Polymer Rheology", 1987, Springer, New York.